Langmuir

Letter

pubs.acs.org/Langmuir

DNA-Mediated Electron Transfer in DNA Duplexes Tethered to Gold Electrodes via Phosphorothioated dA Tags

Rui Campos,[†,‡] Alexander Kotlyar,[§] and Elena E. Ferapontova*[,†,‡]

[†]Interdisciplinary Nanoscience Center (iNANO) and [‡]Center for DNA Nanotechnology (CDNA) at iNANO, Science and Technology, Aarhus University, Gustav Wieds Vej 14, 8000 Aarhus, Denmark

[§]Department of Biochemistry and Molecular Biology, George S. Wise Faculty of Life Sciences and The Center of Nanoscience and Nanotechnology, Tel Aviv University, Ramat Aviv 69978, Israel

Supporting Information

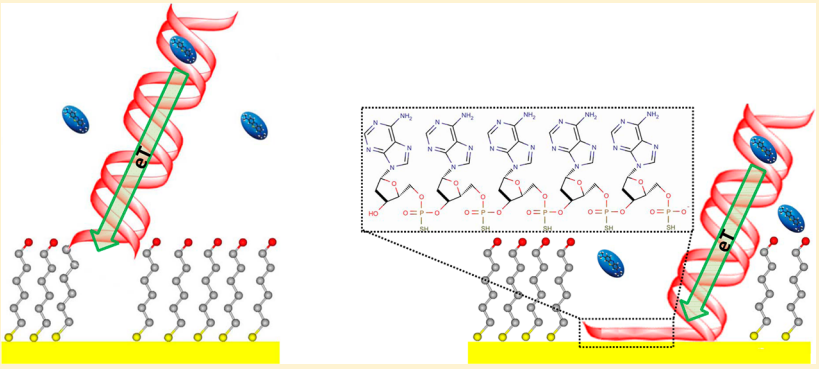

ABSTRACT: The efficiency of DNA-based bioelectronic devices strongly depends on the way DNA molecules are linked to the electronic component. Commonly, DNA is tethered to metal electrodes via an alkanethiol linker representing an additional barrier for electron transport. Here we demonstrate that the replacement of the alkanethiol linker for a phosphorothioated adenosine tag increases the rate of DNA-mediated electron transfer (ET) up to 259 s^{-1}, representing the highest hitherto reported rate of electrochemically-modulated ET, and improves the stability of DNA-electrode surface binding. Both results offer pronounced technological and scientific benefits for DNA-based electronics.

INTRODUCTION

Unique biorecognition and electronic properties of DNA self-assemblies offer challenging applications of this natural nanoscale material in bioelectronics, nanorobotics, sensor and actuator systems, and a number of other nanotechnological applications.[1] Coupled with electrochemistry, they allowed the development of genosensors, the analysis of single nucleotide polymorphism (SNP),[2−4] and the study of electron transport in electrode-tethered DNA.[5−13] These studies, involving either redox-probe-conjugated DNA duplexes or those with intercalated redox probes, are of particular importance both to understanding the fundamentals of electron transfer (ET) reactions proceeding in the electrode-tethered DNA and the design and development of advanced genosensor technologies.

The electrochemical interrogation of DNA tethered to electrodes is routinely performed with DNA chemisorbed onto gold electrodes via an alkanethiol linker introduced either at the 3′ or 5′ end of the DNA molecule.[5−8,10,13−16] The stability and organization of such DNA self-assemblies on gold depend on the strength of thiol-Au binding (35−40 kcal mol^{-1})[17] and may be modulated by the introduction of multiple thiol groups into the DNA sequence.[18] An improved stability of DNA−electrode binding may be also achieved by covalent coupling of the correspondingly modified DNA to activated carbon materials[19] and chemically modified silicon.[20]

From a fundamental point of view, the gold electrode−DNA alkanethiol linkage introduces an additional barrier for DNA-mediated ET, with ET rates exponentially decreasing with the increasing length of the alkane chain bridging the DNA strand and the electrode.[7] The experimentally observed decay in the ET rate constant, k_s, with the increasing number of alkanethiol methylene spacers, n, was consistent with the tunneling parameter β of 1.0 per methylene unit of the alkanethiol linker, fitting the general equation

$$k_s = k_s^{n=0} \exp(-\beta n) \quad (1)$$

where the ET rate constant extrapolated to a zero length of the linker, $k_s^{n=0}$, was estimated to be 10^8−10^9 s^{-1}.[7] Impeded ET is also expected for any other modification involving a spacer between DNA and the electrode-tethered functional group, and a removal of the spacer should then result in improved ET rates, theoretically approaching $k_s^{n=0}$. In addition, long

Received: July 14, 2014
Revised: September 17, 2014
Published: September 29, 2014

alkanethiol chains may promote the free motion of the DNA duplex and its bending to the electrode surface, and this bending may provide ET pathways alternative to the DNA-mediated ET.[8]

Practically, the necessity of the synthetic introduction of the alkanethiol linker into the DNA sequence by automated DNA synthesis is the most inconvenient because it restricts the length of the modified sequence just to those synthetically available (not exceeding 100 nucleotides) and is quite expensive.

Recently, phosphorothioates, or *S*-oligos, where one of the nonbridging oxygens is replaced by sulfur (Figure 1C), have been used for the fabrication[21] and modification[22] of nanoparticles and surface modification by DNA.[23,24] Phosphorothioated residues can be easily introduced enzymatically into DNA molecules of any length, making it possible to probe the conductivity of double-stranded molecules longer that those obtained by a solid-phase synthesis.[24]

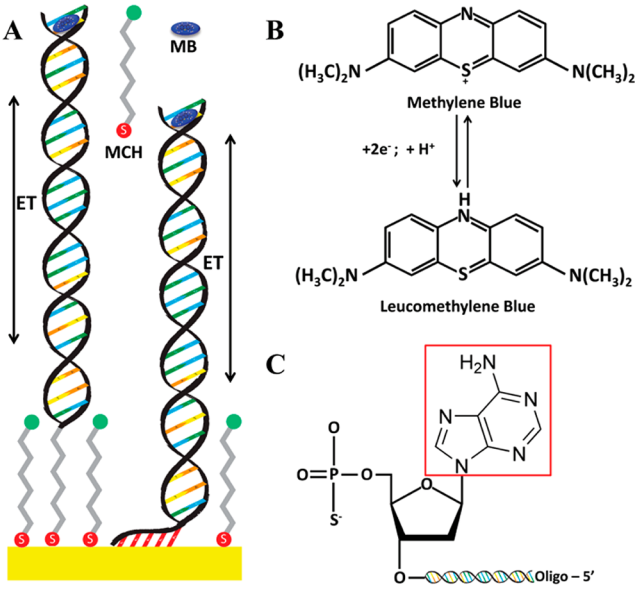

Figure 1. (A) Schematic representation of the DNA-mediated ET through the DNA duplex immobilized onto the gold electrode via the C6 alkanethiol linker and dA_5* tag. (B) Redox reaction of methylene blue at pH >6. (C) Chemical structure of phosphorothioated adenosine.

In the present work, the electronic properties of DNA duplexes tethered to gold electrodes were studied with 20-mer DNA duplexes self-assembled onto the electrodes via either a five phosphorothioated adenosine tag (dA_5*) or an alkanethiol linker (C6), both placed at the DNA 3′-end (Figure 1 and SI). The removal of the alkane linker (of approximately 1.1 nm length) was expected to result in improved DNA-mediated ET rates sought in bioelectronics. The efficiency of DNA-mediated ET through the duplex was evaluated by electrochemical analysis of the kinetics of ET between the electrode and the methylene blue (MB) redox probe intercalated into the DNA. The two DNA immobilization strategies (via C6 and dA_5*) were compared in terms of the electronic properties of the electrode-tethered DNA duplexes and the stability of DNA binding.

EXPERIMENTAL SECTION

Materials. All DNA sequences (probe 5′-GTT GTG CAG CGC CTC ACA AC-3′, complementary 5′-GTT GTG AGG CGC TGC ACA AC-3′, and SNP-containing 5′-GTT GTG AGG CAC TGC ACA AC-3′ DNAs) were synthesized by Metabion Int., Germany. Probe DNA had either a C6-disulfide (C6-DNA) or dA_5* tag (dA_5*-DNA) at the 3′-end.

Electrode Modification with DNA. Electrochemically clean electrodes (CH Instruments, USA; diameter 2 mm) were incubated overnight in a 10 μM dsDNA solution in 10 mM phosphate buffer solution (PBS), pH 7.0, containing 50 mM NaCl and 0.1 M $MgCl_2$. To eliminate nonspecific DNA adsorption, the electrode surface was then additionally treated with mercaptohexanol (MCH); this procedure was important both for C6-DNA- and dA_5*-DNA-electrode modification (Figure S1, SI). The DNA surface coverage, determined by assay with 0.2 mM $Ru(NH_3)_6^{3+}$,[25] was referred to the electrochemically active electrode surface area of 0.055 ± 0.005 cm^2.

Instrumentation. Cyclic voltammetry and square wave voltammetry measurements were performed in a three-electrode cell made of dark glass. An Ag/AgCl (3.5 M KCl) electrode and a Pt flag (1 cm^2) were the reference and auxiliary electrodes, respectively. For more details, please refer to the SI.

RESULTS AND DISCUSSON

ET was studied under conditions of loosely packed DNA films to avoid interactions between neighboring DNA duplexes shown to affect ET kinetics of DNA-interacting redox species.[16] Indeed, consistent with earlier reports,[16] with increasing DNA surface coverage, the electrode−MB ET rates apparently decreased and the overall ET process became complicated, as can be followed from the decreased intensity and distorted symmetry of the normalized MB peak currents, which are particularly pronounced for C6-DNA (Figure S3, SI). Though MB is a well-known DNA intercalator,[2] its intercalative binding is not strong, and when not present in solution, MB is easily lost from the DNA duplex. The electrochemistry of such a weakly adsorbed species is dramatically affected by the DNA surface coverage, very likely through its effect on the DNA−MB interactions and equilibrium between the MB species intercalated into DNA and those present in solution.[16] The DNA conformational changes in tightly packed DNA films affecting the ET rates may also not be excluded. Thus, to avoid such a detrimental effect of DNA−DNA neighboring interactions, most of the studies in the present work were performed in loosely packed DNA films, with noninteracting free-standing DNA molecules tethered to electrodes.

For identical conditions of immobilization, the surface coverage of DNA immobilized via dA_5* did not exceed that of DNA immobilized via the C6 linker, which may also be connected to the dA_5* linker working as a negatively charged spacer between the adsorbed DNA molecules (Table 1, Figure S3, SI). Because of the multiple sulfur−gold attachment points, dA_5* binding to gold improved the stability of the DNA layer. Only 15 ± 2% of the DNA molecules desorbed from the electrode surface after 4 days of storage in PBS versus 23 ± 2% detected for the C6-tethered DNA (Figure S2, SI). A similar

Table 1. Surface Coverage, Γ, and the ET Rate Constant, k_s, Estimated for Perfectly Matched (PM) and SNP-Containing dsDNA Immobilized onto the Gold Electrodes via C6 and dA_5* Linkers

	Γ_{DNA}/pmol cm^{-2}	k_s/s^{-1} (CV)	k_s/s^{-1} (SWV)
$C6_{PM}$	2.9 ± 0.1	107 ± 17	162 ± 9
$C6_{SNP}$	1.7 ± 0.2	88 ± 11	135 ± 8
$dA_5{}^*_{PM}$	1.3 ± 0.4	177 ± 21	259 ± 11
$dA_5{}^*_{SNP}$	0.9 ± 0.1	157 ± 16	197 ± 10

dx.doi.org/10.1021/la502766g | *Langmuir* 2014, 30, 11853−11857

effect was earlier observed with a DNA-trithiol self-assembled monolayer, with ~20% of it desorbing from the gold surface in 5 days versus ~30% shown for the C6-tethered DNA.[26]

A pronounced couple of redox peaks correlated with the electrochemistry of MB and centered at −225 ± 6 and −235 ± 11 mV, for C6 and dA_5*-linked DNA, respectively, could be seen in cyclic voltammograms (CV) and square wave voltammograms (SWV) recorded with the DNA-modified gold electrodes (Figure 2). On average, a −10 mV potential

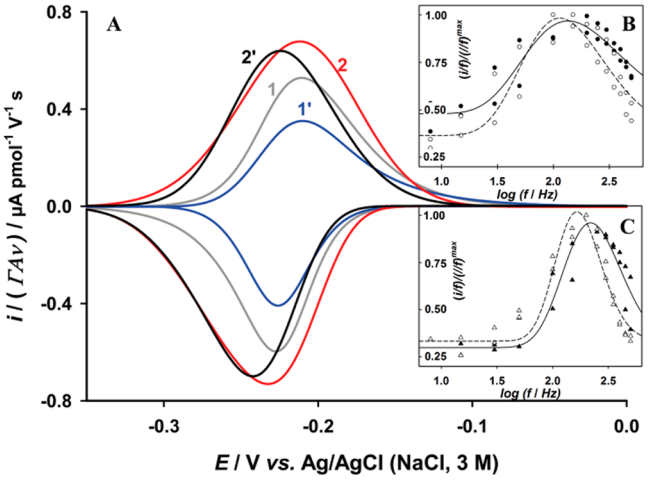

Figure 2. (A) Representative background-corrected cyclic voltammograms, recorded with DNA-modified gold electrodes in 10 mM PBS, pH 7, in the presence of 0.1 μM MB, normalized for the surface coverage Γ (pmol cm^{-2}), scan rate ν (V s^{-1}), and electrode area A (cm^2) for the C6 and dA_5* linkers used. (1) $C6_{PM}$, (1′) $C6_{SNP}$, (2) dA_5*_{PM}, and (2′) dA_5*_{SNP}. (B, C) Dependence of the normalized relation (i/f) between the SWV peak currents i and the frequency f in semilogarithmic coordinates. Full symbols and lines refer to PM, and empty symbols and dashed lines refer to SNP. (B) C6 linkage and (C) dA_5* linkage; all other conditions are the same as in A.

shift was observed when changing from C6- to dA_5*-linked DNA, which may be connected to the negatively charged dA_5* linker introducing an extra charge into the electric double layer. The current signals were consistent with the rate-limiting heterogeneous ET (diffusionless electrochemistry, Figures S4 and S5, SI). Thus, the ET rate constant, k_s, was evaluated by the Laviron theory for adsorbed species,[27] and according to the Komorsky−Lovrić−Lovrić formalism,[28] it was earlier shown to give more precise data on ET kinetics for the case of weakly adsorbed species[10,16] (details in the SI).

As can be seen from Figure 2 and Table 1, the DNA linkage to gold electrodes via the dA_5* tag resulted in an increased rate of DNA-mediated ET of up to 259 s^{-1} as compared to 162 s^{-1} observed with the C6-tethered DNA. Those are the highest hitherto reported DNA-mediated ET rates detected electrochemically. Interestingly, the ET rates in the absence of the alkanethiol linker appear not to be as high as might be expected if the electron tunneling through the linker is considered to be a rate-limiting step.[7] The theoretical ET rate constant extrapolated to a zero-length linker value was estimated to be on the order of 10^8−10^9 s^{-1},[7] which is far above the values detected here. The involvement of alternative mechanisms restricting the ET rate should therefore be taken into account, e.g., the electrochemistry of the MB redox probe that generally undergoes a $2e^-/1H^+$ transfer reaction[29] (Figure 1B) and is switching to a one ET mechanism at high potential scan rates used here for the analysis of ET kinetics. Therewith, interference from protonation and second ET steps may not be totally eliminated.

Because lateral (not DNA-mediated) ET cannot be a priori excluded, e.g., for nonspecifically adsorbed DNA lying flat on the electrode surface, to confirm further the ET mechanism via the DNA duplex, the effect of SNP on the ET rate has been studied. The presence of SNP in the DNA duplex (G replacement for A in the complementary DNA) decreased the k_s an average of 18% for both C6 and dA_5* linkers (Table 1, Figure 2, and Figures S4 and S5 in the SI). This confirms that ET from the electrode to the intercalated dye (Figure 1) occurs via the DNA π-stacked duplex and is not assisted by lateral interactions between the electrode and electrode-tethered DNA double strands.[9,10] This conclusion is consistent with the upright orientation of the negatively charged DNA strands at the electrode surface within the negative potential window used in MB studies,[10,11,30] and such an orientation was also assisted by backfilling the DNA monolayer with a short-chain alkanethiol eliminating any unspecific adsorption of DNA (Figure S1, SI).

It is interesting that, consistent with earlier reports on covalently attached intercalators,[9] the presence of SNP apparently decreased the current signal intensity in the C6-DNA as compared to that in the perfectly matched duplex, whereas a much smaller decrease in the peak current signal, accompanied by a ca. −12 mV shift in the peak potentials (versus −4 mV detected for the C6-DNA), could be followed for the $dA*_5$-DNA duplex (Figure 2). Such a decrease in the peak current signal cannot be explained on the basis of the same mechanism of ET and the same number of intercalated species (such as for covalently attached intercalators)[9] assumed for SNP-containing and perfectly matched duplexes unless the mechanism of ET through the DNA duplex changes in the presence of SNP. Then, the removal of the C6 linker, which was earlier shown to limit the overall DNA-mediated ET reaction,[7] should change the limiting step of the reaction, and that is translated through the peak current and potential variations.

Finally, the ET rate constants were evaluated over a broader range of DNA surface coverages by both CV and SWV techniques (Figures 3 and S3, SI). Independently of the techniques used, the general difference in the ET rate constants remained at higher DNA surface coverages and also at Γ_{DNA} approaching 40% of the theoretical C6-DNA monolayer (around 8.6 pmol cm^{-2}).[5] In the case of the dA_5*-DNA films, the maximum surface coverage obtained under identical conditions of immobilization was 3.5 pmol cm^{-2}, which was less than that of C6-DNA and resulted from the spatial separation of the DNA molecules at the electrode surface preconditioned by the dA_5* linker. For comparable surface coverages (3.5 and 3.6 pmol cm^{-2} for the dA_5* and C6 linkers, correspondingly), the dA_5* linker still provided ET rates ~20% higher than ET rates provided by the C6 linker. Along with that, as expected, the ET rate constants tend to decrease with the increasing population of the DNA molecules at the electrode surface, thus affecting the ET kinetics similarly to other systems that involve the weak adsorption of redox species to DNA duplexes.[16] For densely packed C6-DNA monolayers, k_s approached the value of 89 ± 14 s^{-1} shown with DNA-intercalated daunomycin and compact SAMs of DNA tethered to the surface through the C6 linker.[7]

dx.doi.org/10.1021/la502766g | Langmuir 2014, 30, 11853−11857

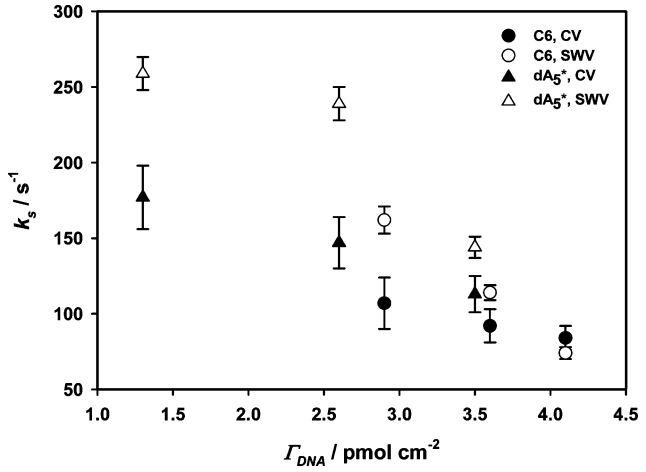

Figure 3. Dependence of the DNA surface coverage, Γ_{DNA} (pmol cm^{-2}) on k_s for the (circles) C6 and (triangles) dA_5* linkers. Full symbols refer to the CV analysis, and empty symbols refer to the SWV analysis. (The error in the CV data is based on different scan rates, and the error in the SWV data is based on the curve fitted with a convergence of over 93%, Figure S3, SI.)

OUTLOOK

As demonstrated here, electronic coupling of DNA to electrodes via the phosphorothioated adenosine tag, which can easily and inexpensively be introduced into the DNA molecule by biochemical synthesis, offers several advantages in DNA electronic applications as compared to the commonly used alkanethiol linker. First, the ET properties of the electrode-tethered DNA and the stability of DNA–gold electrode binding are essentially improved as a result of the removal of the alkane spacer representing an additional ET barrier and multiple dA* tag–gold attachment points. Second, because the ET sensitivity for single nucleotide polymorphism is conserved, DNA immobilization via the dA* tag provides DNA molecular orientation at the electrode, which is essential for DNA-mediated ET phenomena. Finally, the possibility of dA* tag introduction into DNA sequences of any length removes the automated DNA synthesis restriction on the length of the DNA sequence being modified with alkanethiol linkers. That allows fundamental studies of DNA-mediated ET within long genomic DNA sequences and the design of cost-effective genosensors and aptasensors based on oligonucleotide sequences longer than those synthetically available, both being of the highest technological and scientific importance.

ASSOCIATED CONTENT

Supporting Information

Experimental details, data on the DNA surface coverage, and representative CVs and SWVs and their analytical processing equations. This material is available free of charge via the Internet at http://pubs.acs.org.

AUTHOR INFORMATION

Corresponding Author

*E-mail: elena.ferapontova@inano.au.dk.

Notes

The authors declare no competing financial interest.

ACKNOWLEDGMENTS

The work was supported by the Danish National Research Foundation (DNRF) through their support of the CDNA, grant number DNRF81.

REFERENCES

(1) Kjems, J.; Ferapontova, E.; Gothelf, K.: Nucleic Acid Nanotechnology Preface. In *Nucleic Acid Nanotechnology*; Kjems, J., Ferapontova, E., Gothelf, K., Eds.; Nucleic Acids and Molecular Biology Series; Springer-Verlag: Germany, 2014; Vol. *29*; pp IX–X.

(2) Boon, E. M.; Ceres, D. M.; Drummond, T. G.; Hill, M. G.; Barton, J. K. Mutation detection by electrocatalysis at DNA-modified electrodes. *Nat. Biotechnol.* **2000**, *18*, 1096–1100.

(3) Fan, C. H.; Plaxco, K. W.; Heeger, A. J. Electrochemical interrogation of conformational changes as a reagentless method for the sequence-specific detection of DNA. *Proc. Natl. Acad. Sci. U.S.A.* **2003**, *100*, 9134–9137.

(4) Satterwhite, J. E.; Pugh, A. M.; Danell, A. S.; Hvastkovs, E. G. Electrochemical detection of anti-benzo[a]pyrene diol epoxide DNA damage on TP53 codon 273 oligomers. *Anal. Chem.* **2011**, *83*, 3327–3335.

(5) Hartwich, G.; Caruana, D. J.; de Lumley-Woodyear, T.; Wu, Y. B.; Campbell, C. N.; Heller, A. Electrochemical study of electron transport through thin DNA films. *J. Am. Chem. Soc.* **1999**, *121*, 10803–10812.

(6) Long, Y. T.; Li, C. Z.; Sutherland, T. C.; Chahma, M.; Lee, J. S.; Kraatz, H. B. A comparison of electron-transfer rates of ferrocenoyl-linked DNA. *J. Am. Chem. Soc.* **2003**, *125*, 8724–8725.

(7) Drummond, T. G.; Hill, M. G.; Barton, J. K. Electron transfer rates in DNA films as a function of tether length. *J. Am. Chem. Soc.* **2004**, *126*, 15010–1.

(8) Anne, A.; Demaille, C. Electron transport by molecular motion of redox-DNA strands: Unexpectedly slow rotational dynamics of 20-mer ds-DNA chains end-grafted onto surfaces via C(6) linkers. *J. Am. Chem. Soc.* **2008**, *130*, 9812–9823.

(9) Slinker, J. D.; Muren, N. B.; Renfrew, S. E.; Barton, J. K. DNA charge transport over 34 nm. *Nat. Chem.* **2011**, *3*, 228–233.

(10) Abi, A.; Ferapontova, E. E. Unmediated by DNA Electron Transfer in Redox-Labeled DNA Duplexes End-Tethered to Gold Electrodes. *J. Am. Chem. Soc.* **2012**, *134*, 14499–14507.

(11) Farjami, E.; Campos, R.; Ferapontova, E. E. Effect of the DNA End of Tethering to Electrodes on Electron Transfer in Methylene Blue-Labeled DNA Duplexes. *Langmuir* **2012**, *28*, 16218–16226.

(12) Mie, Y.; Kojima, N.; Kowata, K.; Komatsu, Y. End-tether structure of DNA alters electron-transfer pathway of redox-labeled oligo-DNA duplex at electrode surface. *Chem. Lett.* **2012**, *41*, 62–64.

(13) Huang, K. C.; White, R. J. Random walk on a leash: a simple single-molecule diffusion model for surface-tethered redox molecules with flexible linkers. *J. Am. Chem. Soc.* **2013**, *135*, 12808–12817.

(14) Herne, T. M.; Tarlov, M. J. Characterization of DNA probes immobilized on gold surfaces. *J. Am. Chem. Soc.* **1997**, *119*, 8916–8920.

(15) Petrovykh, D. Y.; Kimura-Suda, H.; Whitman, L. J.; Tarlov, M. J. Quantitative analysis and characterization of DNA immobilized on gold. *J. Am. Chem. Soc.* **2003**, *125*, 5219–5226.

(16) Campos, R.; Ferapontova, E. E. Electrochemistry of weakly adsorbed species: Voltammetric analysis of electron transfer between gold electrodes and Ru hexaamine electrostatically interacting with DNA duplexes. *Electrochim. Acta* **2014**, *126*, 151–157.

(17) Ulman, A. Formation and structure of self-assembled monolayers. *Chem. Rev.* **1996**, *96*, 1533–1554.

(18) Johnson, R. P.; Gale, N.; Richardson, J. A.; Brown, T.; Bartlett, P. N. Denaturation of dsDNA immobilised at a negatively charged gold electrode is not caused by electrostatic repulsion. *Chem. Sci.* **2013**, *4*, 1625–1632.

(19) Hansen, M. N.; Farjami, E.; Kristiansen, M.; Clima, L.; Pedersen, S. U.; Daasbjerg, K.; Ferapontova, E. E.; Gothelf, K. V. Synthesis and application of a triazene-ferrocene modifier for

immobilization and characterization of oligonucleotides at electrodes. *J. Org. Chem.* **2010**, *75*, 2474−2481.
(20) Lamture, J. B.; Beattie, K. L.; Burke, B. E.; Eggers, M. D.; Ehrlich, D. J.; Fowler, R.; Hollis, M. A.; Kosicki, B. B.; Reich, R. K.; Smith, S. R.; Varma, R. S.; Hogan, M. E. Direct-Detection of Nucleic-Acid Hybridization on the Surface of a Charge-Coupled-Device. *Nucleic Acids Res.* **1994**, *22*, 2121−2125.
(21) Junghans, M.; Kreuter, J.; Zimmer, A. Phosphodiester and phosphorothioate oligonucleotide condensation and preparation of antisense nanoparticles. *BBA-Protein Struct. Mol. Enzymol.* **2001**, *1544*, 177−188.
(22) Lubitz, I.; Kotlyar, A. Self-Assembled G4-DNA-Silver Nanoparticle Structures. *Bioconjugate Chem.* **2011**, *22*, 482−487.
(23) Ihara, T.; Nakayama, M.; Murata, M.; Nakano, K.; Maeda, M. Gene sensor using ferrocenyl oligonucleotide. *Chem. Commun.* **1997**, 1609−1610.
(24) Ghabboun, J.; Sowwan, M.; Cohen, H.; Molotsky, T.; Borovok, N.; Dwir, B.; Kapon, E.; Kotlyar, A.; Porath, D. Specific and efficient adsorption of phosphorothioated DNA on Au-based surfaces and electrodes. *Appl. Phys. Lett.* **2007**, *91*, 173101.
(25) Steel, A. B.; Herne, T. M.; Tarlov, M. J. Electrochemical quantitation of DNA immobilized on gold. *Anal. Chem.* **1998**, *70*, 4670−4677.
(26) Phares, N.; White, R. J.; Plaxco, K. W. Improving the stability and sensing of electrochemical biosensors by employing trithiol-anchoring groups in a six-carbon self-assembled monolayer. *Anal. Chem.* **2009**, *81*, 1095−1100.
(27) Laviron, E. General expression of the linear potential sweep voltammogram in the case of diffusionless electrochemical systems. *J. Electroanal. Chem.* **1979**, *101*, 19−28.
(28) Komorsky-Lovric, S.; Lovric, M. Kinetic measurements of a surface-confined redox reaction. *Anal. Chim. Acta* **1995**, *305*, 248−255.
(29) Svetlicic, V.; Clavilier, J.; Zutic, V.; Chevalet, J. Electrochemical Evidence of 2-Dimensional Surface-Compounds of Heterocyclic Molecules at Sulfur-Covered Gold and Platinum.1. Methylene-Blue. *J. Electroanal. Chem.* **1991**, *312*, 205−218.
(30) Rant, U.; Arinaga, K.; Fujita, S.; Yokoyama, N.; Abstreiter, G.; Tornow, M. Dynamic electrical switching of DNA layers on a metal surface. *Nano Lett.* **2004**, *4*, 2441−2445.